aerospace

MDPI

Article

Aerodynamic Analysis of Blade Stall Flutter Prediction for Transonic Compressor Using Energy Method

Ali Arshad * and Akshay Murali

Aeronautics, Space Engineering and Transport Institute, Faculty of Civil and Mechanical Engineering, Riga Technical University, LV-1048 Riga, Latvia

* Correspondence: ali.arshad@rtu.lv

Abstract: In this study, stall flutter onset prediction in a transonic compressor is carried out using the (uncoupled) energy method with Fourier transform. As the study is conducted computationally using computational fluid dynamics (CFD)-based simulations, the energy method was employed due to its higher computational efficiency by implementing the one-way FSI (Fluid Structure Interaction) model. The energy method is relatively uncommon for determining the aerodynamic damping and flutter prediction, specifically in blade stall conditions for the 3D blade passages. The NASA Rotor 67 was chosen for the validation of the study due to the availability of a wide range of experimental data. A flutter prediction analysis was performed computationally using CFD for the two-blade passages of the rotor in the peak efficiency and stall regions. Prior to this, the modal analysis on the prestressed blade was conducted, considering the centrifugal effects. The modal analysis provided accurate blade frequency and amplitude, which were the inputs of the flutter analysis. The first three modes of blade resonance were studied with a range of nodal diameters within near-peak efficiency and stall regions. The energy method implemented in this study for the flutter analysis was successfully able to predict the aerodynamic damping coefficients of the first three modes for a range of nodal diameters from the periodic-unsteady solution of the defined blade oscillation within the regions of interest (peak efficiency and stall point). The results of the study confirm the rotor blade's stability within the near-peak region and, most importantly, the prediction of the flutter onset in the stall region. The study concluded that the computationally inexpensive and time-efficient energy method is capable of predicting the stall flutter onset. In the future, further validations of the energy method and investigations related to flow mechanism of stall flutter onset are planned.

Keywords: energy method; Fourier transform; turbulent blade row; aerodynamic damping; nodal diameter; inter-blade phase angle; stall flutter

Citation: Arshad, A.; Murali, A. Aerodynamic Analysis of Blade Stall Flutter Prediction for Transonic Compressor Using Energy Method. *Aerospace* **2024**, *11*, 815. https://doi.org/10.3390/aerospace11100815

Academic Editor: Bosko Rasuo

Received: 2 September 2024
Revised: 28 September 2024
Accepted: 29 September 2024
Published: 6 October 2024

1. Introduction

The demand for fuel-efficient, lightweight, and high-performance commercial aircraft engines has driven the manufacturers towards designing lighter blades with higher pressure ratios per stage making them prone to flutter. This aeroelastic instability is mostly seen in the first stages of the compressor and the last stages of the turbine. While the rotating stall of a compressor has been studied extensively from the aerodynamic perspective, the study of flutter/aeroelasticity provides another view for understanding the complex flow phenomenon of compressor stalls.

Flutter is a self-excited and self-sustained aeroelastic instability phenomenon where the unsteady pressure field of the flow caused due to the vibration of the structure adds energy to the structure, which is beyond the damping capacity of the system, causing an exponential increase in the oscillation amplitude. For example, in an ideal stable system, the aerodynamic forces acting on a structural element exposed to fluid flow are balanced out by the inertial and elastic forces, dissipating the energy imparted by the fluid to the structure. In turbomachinery, flutter occurs when energy imparted by the flow on the blade

over a cycle due to the blade's vibration at the natural frequency is sufficient to overcome the damping capability of the blade.

Flutter due to its inherent nonlinear nature and dependency on both the aerodynamic and structural characteristics of the blade made computational fluid dynamics (CFD) difficult to implement and computationally expensive. The advancements in integrated CFD methods and affordable computational power have given headway to significant progress in developing methods for flutter prediction in turbomachinery. Casoni and Benini [1] in their study divided the existing methods for predicting flutter in turbomachinery into two broad categories, namely the classical method and the coupled method. In the classical method, the fluid and structural domain is computed separately, while in the coupled method the fluid and structural domains are considered as a single domain and there is a transfer of data between them, i.e., any changes in the fluid affect the structure and vice versa. Several studies [2–13] have been conducted using the uncoupled and coupled methods for accurately predicting flutter in turbomachinery. For example, the study by Zheng and Yang [2] used a coupled fluid–structure method based on the time-domain solution of the fluid–structure where the aerodynamic and structural equations were marched simultaneously to predict flutter of a transonic fan. The method used was not only able to predict the stability of the blade but also able to compute the amplitude and frequency of the vibration. Another example of fully coupled flutter prediction is the study by Chen et al. [3], where fully coupled numerical methodology was developed to calculate the flow-structure interaction and to predict transonic NACA 64A010 airfoil flutter. The study was not only able to capture the limit cycle oscillation (LCO) but also obtained the flutter boundary with the transonic dip. This paper focuses on the use of the unsteady uncoupled energy method to predict the flutter of a transonic compressor in regions of near-peak efficiency and stall. The energy method is a classical method developed by Carta [4] based on calculating the algebraic sum of the work done by the aerodynamic forces on the blade oscillating with a pre-determined amplitude. Even though the fully coupled method is known for its accuracy and ability to capture coupled flutter characteristics, it can be computationally expensive.

The CFD energy method compared to the coupled methods of flutter prediction is efficient, accurate and computationally inexpensive as the fluid and structural domains are treated separately [5,6]. Chahine et al. [5] in their study compared the coupled and decoupled fan flutter prediction methods for varying values of mass ratio and blade stiffness of a transonic three-dimensional rotor. The study concluded that the results of both methods were comparable for all the cases of isolated variation in mass ratio and stiffness from baseline and the decoupled/energy method was able to predict the stability for a maximum frequency shift value of 1.2%. The work done by Li and Sheng [7] checked the extent, to which the energy method could be used to predict stall flutter in a transonic blade, and included a structural model with two degrees of freedom combined with an unsteady aerodynamic model. The stall flutter boundaries for two rotors were predicted with the energy method and were found to agree well with the experimental values. The work by Clark and Hall [8] used a time-linearized Navier–Stokes computational method for predicting the onset of flutter in a viscous flow through a two-dimensional cascade to predict stall flutter by decomposing the flow into a nonlinear spatially varying mean flow with the addition of a small perturbation, and the comparison of the CFD results to experimental values of stall flutter were found to be in agreement.

Based on the above-mentioned literature survey, the main aim of this study is to investigate the application of the energy method for the prediction of stall flutter onset in a transonic compressor. The NASA Rotor 67 transonic compressor was chosen for this analysis due to the wide-range availability of its experimental and CFD data (in literature). The energy method is an uncoupled method of flutter study, which, in fact, is convenient due to its lower consumption of computational resources and time efficiency. In addition, the energy method has already been previously used for flutter prediction; however, the stall-related flutter onset prediction by using the energy method has not been fully addressed. Therefore, in this study, stall flutter onset prediction was carried

out in a stepwise manner. In the first step, a modal analysis was carried out to evaluate the natural frequencies and mode shapes. The modal analysis results (of this study) were compared with the previous studies [9] on the NASA Rotor 67. In the next step, CFD simulations were carried out for the evaluation of the compressor performance, which was close to the experimental results of Strazisar et al. [14,15]. In the final step, transient CFD simulations were performed to determine the blade aerodynamic damping for two cases: (i) near-peak efficiency, (ii) and stall condition. From the obtained values of aerodynamic damping, the system stability was evaluated. At the near-peak compressor efficiency, no flutter-related instability was detected, which was also proven in the previous studies [6,9]; however, for the compressor stall condition, system instability was detected by a negative aerodynamic damping value at a backward-traveling wave (negative nodal diameter). This stepwise compressor stall flutter analysis successfully demonstrated the applicability of the computational inexpensive energy method. Further validations of the stall flutter onset prediction along with the flow phenomenon causing such system instability are planned in the future.

This study is part of the series of current [16–20] and future studies under the European Latvian Council of Science 4R-UAV project and the National Research Program Project: Sports, which is funded by the Ministry of Science and Education of Latvia with the aim to develop innovative and environmentally friendly aerospace and sports equipment at Riga Technical University, Latvia.

2. Methodology

In this study, the flutter analysis is carried out using the double-passage energy method. The analysis was performed in the following steps:

2.1. Rotor Design and Specifications: NASA Rotor 67

The NASA Rotor 67 is a low-aspect-ratio axial fan rotor with twenty-two blades and is the first rotor of a two-stage transonic compressor. The Rotor 67 has been a popular model for past flutter studies. The availability of the experimental and CFD-based research literature of the Rotor 67 provides a good comparison for this study. The rotor was designed at a mass flow rate of 33.25 kg/s and a design rotational speed of 16,043 rpm, resulting in an inlet tip Mach number of 1.38. Figure 1 illustrates the NASA Rotor 67 model designed in Ansys SpaceClaim while Table 1 summarizes the rotor's main specifications. The laser anemometer survey by Strazisar et al. [14,15] provides in-depth experimental data for the compressor performance map, including near-peak and near-stall conditions, which are used in this study to validate the numerical results.

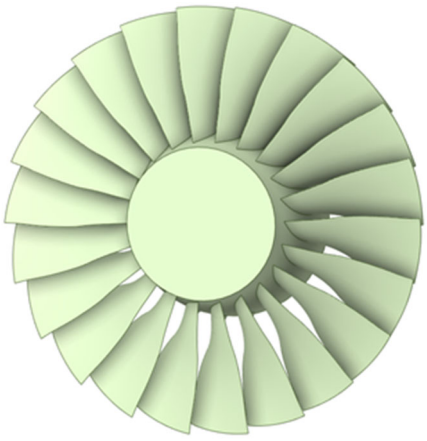

Figure 1. NASA Rotor 67 model designed for flutter onset analysis.

Table 1. NASA Rotor 67 characteristics.

Number of blades	22
Rotor speed	16,043 (RPM)
Tip speed	429 (m/s)
Inlet tip relative Mach number	1.38
Mass flow rate	33.25 (kg/s)
Pressure ratio	1.63
Tip clearance	1.01 (mm)
Blade aspect ratio	1.56
Tip solidity	1.29
Hub solidity	3.11
Inlet hub/tip ratio	0.375
Exit hub/tip ratio	0.478

2.2. Grid Generation

Two different types of mesh were created, i.e., for the structural analysis, and for the CFD analysis. For the structural FEM analysis, the Ansys Mechanical mesh was used to discretize the model into 6000 elements (Figure 2). However, for the fluid flow domain, Ansys TurboGrid was employed to generate grids for steady- and transient-state simulations (Figures 3 and 4).

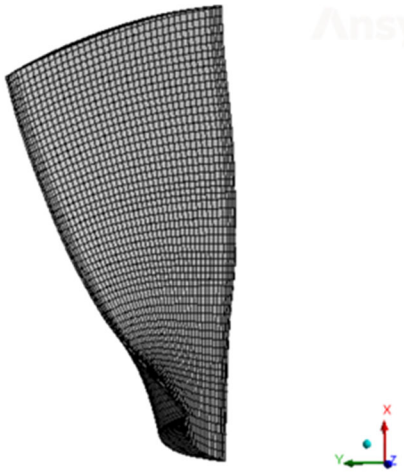

Figure 2. Structural FEM analysis grid for Rotor 67 blade.

Figure 3. Fluid domain mesh for Rotor 67 blade at near hub location.

Figure 4. Fluid domain mesh for Rotor 67 for blade.

For the fluid-flow domain, the mesh was created using the Automated Topology and Meshing (ATM) feature of Ansys TurboGrid. The ATM feature automates the meshing process by inferring the mesh topology based on features like blade passages and hub-to-shroud regions. The single blade was initially modeled in Ansys SpaceClaim, and the flow paths, the inlet, the outlet, the hub, and the shroud were extracted to Ansys TurboGrid for meshing. Three different grid schemes of 271,129 (coarse), 540,677 (medium), and 1,129,793 (fine) elements per blade were created for the mesh independence study. The grids used in previous studies, such as [6,9], were also in the same element count range and proved that the element range was sufficient for the precision of results. Initially, the single-blade passage mesh (including a tip clearance of 1.01 mm) was created, which was later expanded to two-blade passages by using the mesh transformation `function` in Ansys CFX for conducting Fourier transformation.

The mesh independence study was conducted on all three meshes created for the analysis. All three grid schemes predicted similar values for the pressure ratio and efficiency. The mesh independence study is summarized in Tables 2 and 3, where all three grid schemes show a difference of only about 2% for measured efficiency and total pressure ratio. Therefore, the mesh with 540,677 elements was chosen for further steady-state and transient simulations as it satisfies the precision required for the simulation while saving computational costs.

Table 2. Mesh independence comparison for all three grid schemes (total pressure ratio).

Mesh	Total Pressure Ratio (CFD)	Total Pressure Ratio (Experimental)	Pressure Ratio Deviation (%)
Coarse (271,129)	1.649	1.68	1.84
Medium (540,677)	1.6504	1.68	1.76
Fine (1,129,793)	1.6510	1.68	1.72

Table 3. Mesh independence comparison for all three grid schemes (compressor efficiency).

Mesh	Efficiency (CFD) (%)	Efficiency (Experimental) (%)	Efficiency Deviation (%)
Coarse (271,129)	90.89	93	2.32
Medium (540,677)	91.054	93	2.09
Fine (1,129,793)	91.1054	93	2.03

2.3. Computational Scheme

The numerical scheme was divided into two sections. Firstly, the FEM analysis was conducted to obtain the modal shapes of the first three modes. Secondly, the steady-state CFD simulations were conducted to initialize the further transient simulations for the evaluation of the aerodynamic damping of the blade. The transient blade row (TBR) modeling with Fourier transformation was used to run the unsteady blade flutter calculation in Ansys CFX. It is a useful method for CFD simulations to efficiently capture and analyze the flow with periodic nature. The single passage of Rotor 67 was expanded to two passages using the turbo-rotation feature (a requirement for Fourier transform), and a sampling interface was created for the instances that are connected to the periodic boundaries. The interface was set up with a general grid interface (GGI) to accommodate the data transfer across the interface and for its adaptability in handling complex fluid flows. The application of the Fourier transform allowed for a direct imposition of phase shifts between boundaries, facilitating a more straightforward representation of periodic flow phenomena.

Erdos et al. [21] proposed a direct method of imposing the phase-shift boundary, but it required the storage of signal for the full period on the periodic boundaries. The frequency transformation method introduced by He [22] enabled us to avoid storing data on periodic boundaries by using temporal Fourier series decomposition, making it more memory-efficient. Therefore, for this study, the Fourier transformation method in CFX is implemented using a double-passage method, as illustrated in Figure 5. The time shift between the adjacent blades for a blade flutter case and the phase-shifted signals on the periodic boundaries (R1, R2, and R3) are expressed in Equations (1)–(3).

$$\Delta T = \frac{ND}{\omega} \tag{1}$$

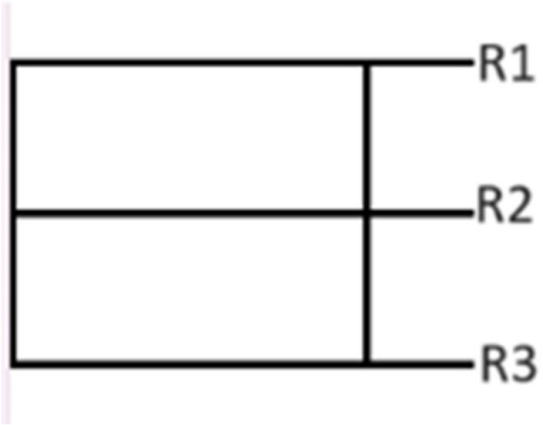

Figure 5. Schematic of the double-passage method.

The signal $f_{R1}(t)$ on R1 is equal to signal on R2 phase shifted by

$$f_{R1}(t) = f_{R2}(t + \Delta T) \approx f'_{R2}(t + \Delta T) \tag{2}$$

The signal $f_{R1}(t)$ on R3 is equal to signal on R2 phase shifted by

$$f_{R1}(t) = f_{R2}(t - \Delta T) \approx f'_{R2}(t - \Delta T) \tag{3}$$

where f'_{R2} is the reconstructed signal from R2 using the accumulated Fourier coefficients on the periodic boundary [23], as shown in Figure 5. In the double-passage method, data are collected at the interface between the two passages, and it provides better convergence and superior quality. The efficiency of this approach lies in its ability to achieve quasi-periodic states in as few as 3–4 cycles [23].

A rotating frame of reference was used for the TBR simulation with the inlet pressure set to the atmospheric pressure of 1 atm and varying outlet pressure to account for the regions of interest (i.e., near-peak and stall regions). The k-ω SST turbulence model [24] known for its accuracy in predicting the onset of flow separation with the reattachment modification (RM) (reattachment production) and Yˆ+ near-wall treatment was employed for this study.

For this study, the periodic displacement option [23] was used to set the transient periodic mesh motion, which repeats at a given frequency to imitate the effect of blade vibrations at the natural frequency of the blade. The mesh imported from the modal analysis containing the cartesian components is extended to the entirety of the compressor row (22 blades) and the extended cartesian coordinates are used to define the displacement of the blades with the scaling factor to define the maximum amplitude of 1.2 mm, which is approximately 1.2% of the chord length (as blade displacements are in the range of up to 2% chord length of the blade). The frequency and the phase angle for the mesh motion is determined by the natural frequency of the mode shape and the Inter-blade Phase Angle (IBPA) to be investigated. The required IBPA is calculated from the nodal diameter using Equation (4).

$$\text{IBPA} = \frac{2\pi \text{ND}}{\text{N}_{\text{BL}}} \tag{4}$$

The time period for the TBR was set as 1/(natural vibration frequency) of the associated mode and the time steps per time period of each nodal diameter was determined by Equation (5).

$$\text{Timesteps} = 4 \times \frac{\text{Number of passages in 360}}{\text{Phase Angle Multiplier}} \tag{5}$$

For a phase angle multiplier (PAM) or nodal diameter of 1, the calculated number of time steps per time period was 88. In addition, the Frequency Filtering feature in Ansys CFX was used to avoid unwanted frequency by setting the Damping scale factor to 1. The TBR simulations are also initialized using the converged steady-state simulations to ensure better accuracy and convergence.

3. Results

The results of the FEM and CFD analyses are presented in this section. At first, the modal analysis was performed, and then a steady-state and transient analysis was performed to observe the onset of the flutter in the compressor blade at peak efficiency and stall condition.

3.1. Modal Analysis

The modal analysis was conducted to obtain the mode shapes of natural frequencies of the NASA Rotor 67 compressor blade. For this, the blade was prestressed by taking into consideration the centrifugal loading at compressor design speed, while the hub was set as a fixture (with 0 DOF). In accordance with the actual manufacturing practices, fully solid titanium blade material was chosen for the analysis. The mechanical properties of the chosen material are given in Table 4, while the obtained first three natural frequencies and the associated mode shapes for the rotor blade are shown in Figures 6–8.

Table 4. Blade material (titanium alloy) properties.

Material Properties	Value	Unit
Young's modules	1.172×10^{12} Pa	Pa
Poisson's ratio	0.3	N/A
Density	4539.5	Kg/m^3

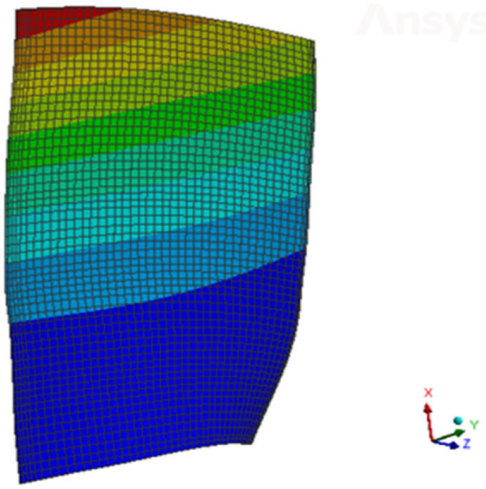

Figure 6. First bending mode of rotor 67.

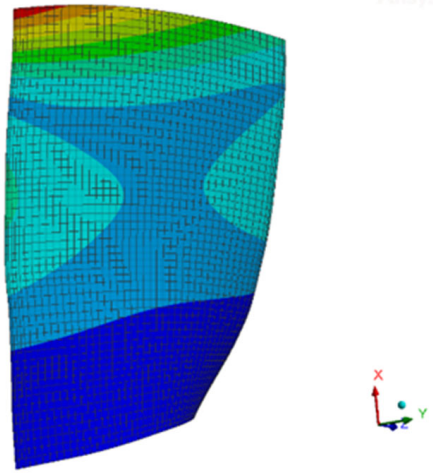

Figure 7. Second bending mode of rotor 67.

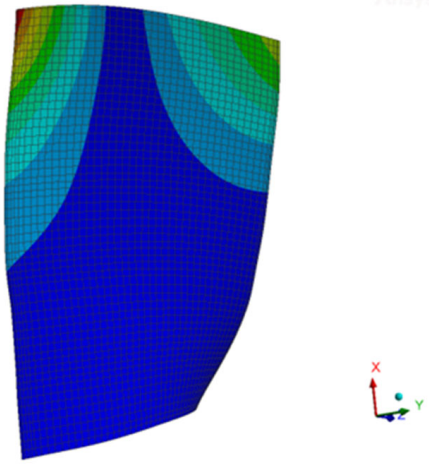

Figure 8. First torsional mode of rotor 67.

It can be observed in Figure 6 for the first bending mode, the leading edge at the blade tip possesses the maximum displacement with an even displacement distribution from hub to tip. Similar to the first mode, the second bending mode also exhibited maximum displacement at the leading edge; however, slightly higher displacement was observed across the width of the blade compared to the first mode, as shown in Figure 7. The third

mode in Figure 8 is the torsional mode with maximum displacement at both the leading and trailing edge. In this study, the obtained natural frequency values were compared (with a maximum deviation of 0.5%) with the frequency values obtained in the study by Ren et al. [9], where the modal analysis was conducted on the NASA Rotor 67 as one of the steps to analyze couple-mode flutter in turbomachinery.

The natural frequency deviations are negligible. The natural frequency values obtained by the authors and the comparitive study are illustrated in Table 5. The mode shapes from the modal analysis of the blade along with its natural frequencies, maximum displacement, and node coordinates (in the form of cartesian co-ordinates) were extracted from Ansys Mechanical using custom APDL code in CSV format to be imposed as mesh motion for the blade in Ansys CFX.

Table 5. Modal analysis and natural frequency comparison.

Mode Number	Natural Frequency (Hz)	Natural Frequencies (from the Study by Ren et al. [9])	Deviation from the Reference Study (%)
1	532.9	533.7	0.15
2	1216	1221.1	0.42
3	1786.6	1795.4	0.49

3.2. CFD Analysis; Compressor Performance

The steady-state CFD analysis was carried out and validated by comparing the compressor performance (obtained in this study) with the experimental data of Strazisar et al. [14,15] for the NASA Rotor 67. The CFD-based steady-state simulations were conducted for a fixed inlet pressure of 1 atm with variable outlet pressure using the k-ω SST turbulence model. Figures 9 and 10 illustrate the compressor performance map where the variations of isentropic efficiency and compressor pressure ratios can be observed against the mass flow rate (normalized for choke conditions). The simulated results satisfy the experimental performance trends with minor deviations (less than 3%). These steady-state numerical validations set the base for initializing the transient cases, which help in achieving a faster convergence of the TBR simulations for predicting the onset of flutter, as discussed in Section 2.3 (Computational Scheme).

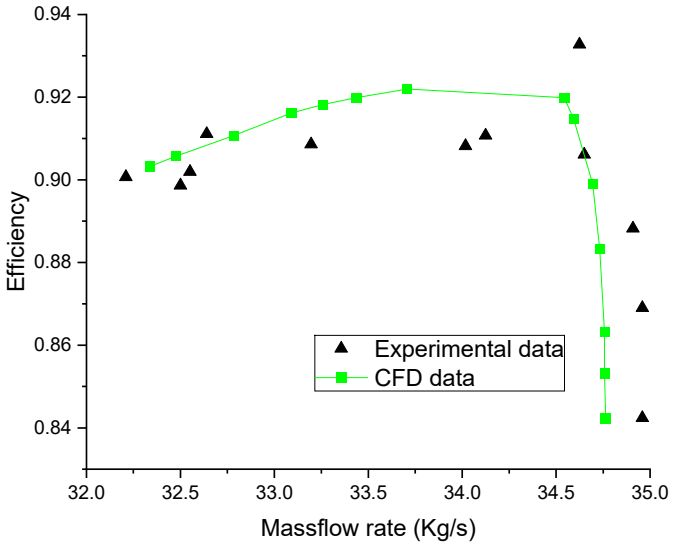

Figure 9. Comparison compressor performance map at design speed.

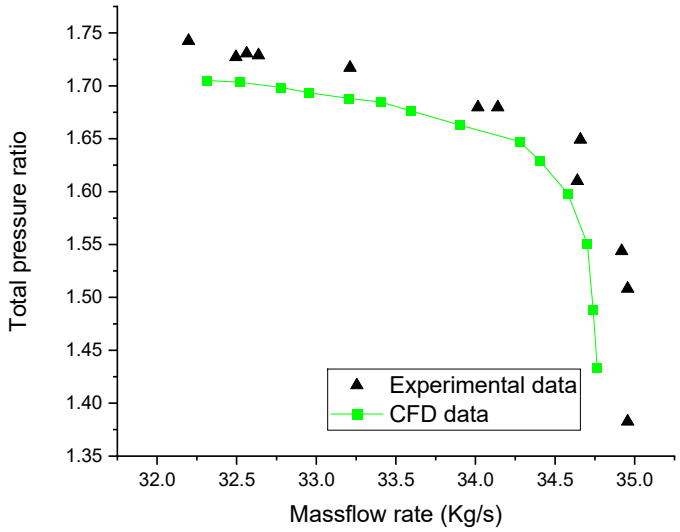

Figure 10. Comparison of compressor total pressure ratio at design speed.

3.3. Flutter Prediction

The TBR modelling with Fourier transformation were used to predict flutter onset in the Rotor 67 for the first three modes of natural vibrations and the nodal diameter in the range of −1 to +4 for compressor near-peak efficiency and stall condition. After the TBR simulation achieved transient periodic solution, the energy method was employed to calculate the aerodynamic damping in order to determine the stability of the system (blade) at each nodal diameter and natural blade vibration frequencies. The work on the blade in each vibration cycle was calculated using Equation (6), where p is the fluid pressure, v is the velocity to the predetermined displacements, A is the surface area of the blade, $\hat{n}$ is the surface normal unit vector, T is the period of one vibration cycle ($\frac{2\pi}{\omega}$), and t_o is the time at the beginning of the vibration cycle [23].

$$W = \int_{t_o}^{t_o+T} \int_A p\vec{v} \times \hat{n} dA dt \tag{6}$$

The nondimensionalized aerodynamic damping was obtained by dividing the work on the blade by the blade kinetic energy.

$$\sigma = \frac{\int_{to}^{t_o+T} \int_A p\vec{v} \times \hat{n} dA dt}{m \times \omega^2 A_{max}^2} \tag{7}$$

where A_{max} is the maximum displacement amplitude and ω is the natural frequency of the mode (considered). In the energy method, positive aerodynamic damping designates a damped system for a particular nodal diameter; on the other hand, a negative value of aerodynamic damping indicates an undamped vibration, which is referred to as an unstable system with the possible onset of flutter.

For this study, flutter onset was analyzed for the two conditions, i.e., near-peak and stall conditions, as explained below:

Aerodynamic damping (near-peak efficiency):

The aerodynamic damping values for the near-peak efficiency region were calculated for the first three natural frequencies of the Rotor 67 (determined by modal analysis in Section 3.1). Figures 11–13 present the aerodynamic damping of the first three natural frequencies for a range of nodal diameters (NDs). For the first mode (Figure 11), the nodal diameter 1 is the least stable (lowest aerodynamic damping) and nodal diameter 4 the most stable (maximum aerodynamic damping). For the second mode (Figure 12), a similar trend was observed i.e., highest damping at ND 4 (most stable) while lowest damping at ND 1 (least stable). In the case of the third mode, ND 0 is most stable while ND 1 is least stable,

as shown in Figure 13. To summarize, all three modes had a consistent trend of positive aerodynamic damping manifesting the overall stability of the rotor in the near-peak region, which means that there was no flutter predicted at the near-peak efficiency. This trend has also been observed in previous studies [6,9].

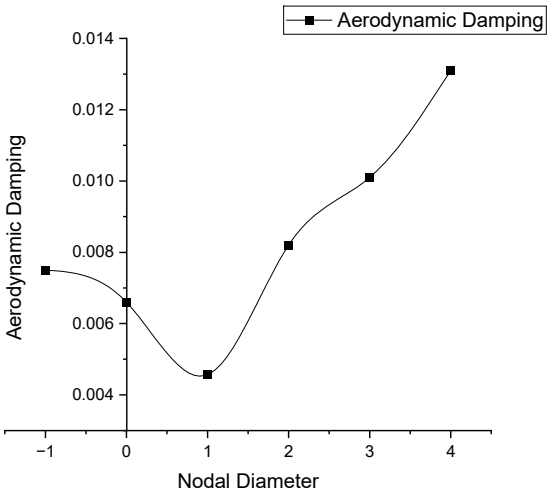

Figure 11. Aerodynamic damping for mode 1.

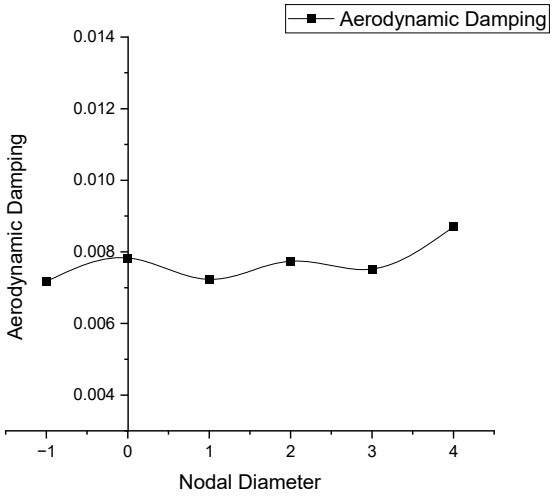

Figure 12. Aerodynamic damping for mode 2.

Aerodynamic Damping (Stall Condition):

The main aim of this study was to predict the onset of flutter in the compressor stall condition. Even though the energy method has been previously used in predicting the compressor blade flutter, its implementation for the stall-related flutter prediction is rather overlooked and rare, as literature mainly covers the flutter prediction in stable compressor-operating regions. Therefore, in this study, the aerodynamic damping values for the stall region were specifically evaluated.

Figures 14–16 illustrate the aerodynamic damping of the first three natural frequencies for a range of NDs. The existence of a negative value of aerodynamic damping can be observed in the first mode at ND −1 (IBPA 16.36 degrees), which, in fact, depicts the system's instability. The other two modes (second and third) show a stable tendency within all considered NDs.

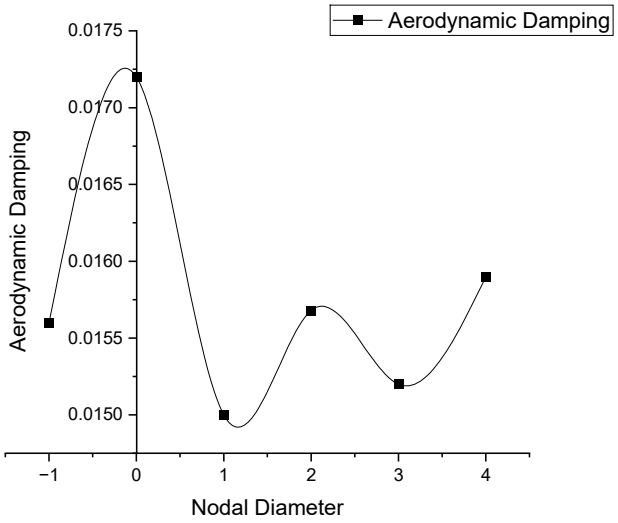

Figure 13. Aerodynamic damping for mode 3.

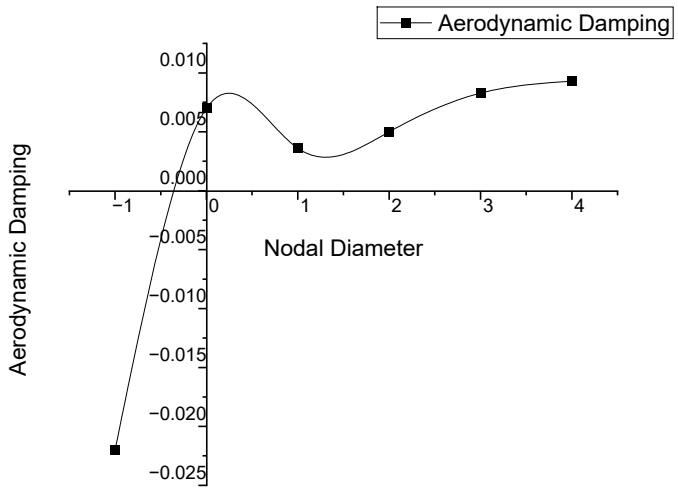

Figure 14. Aerodynamic damping for mode 1.

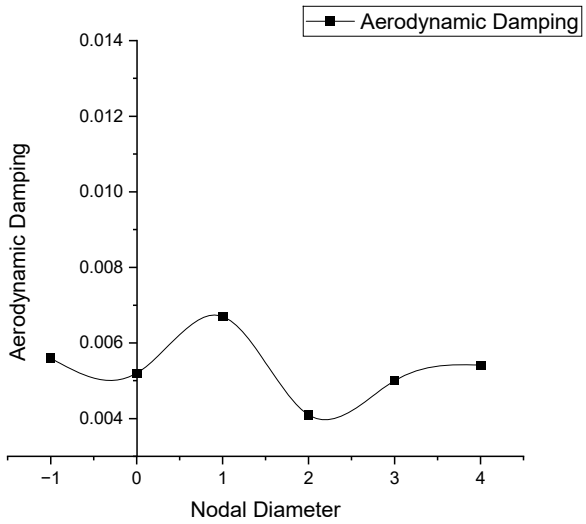

Figure 15. Aerodynamic damping for mode 2.

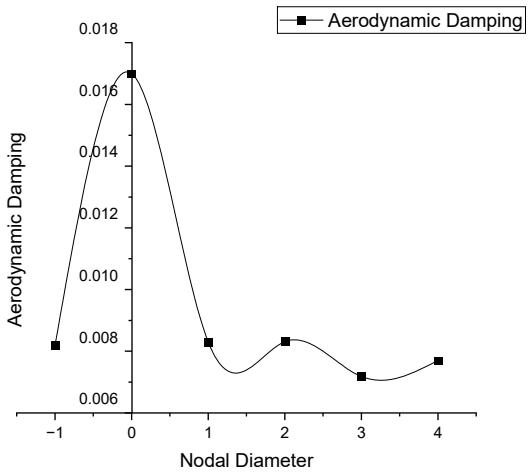

Figure 16. Aerodynamic damping for mode 3.

4. Discussion and Conclusions

This paper explored a relatively "untouched" topic of flutter onset prediction in transonic compressor blade stall conditions using the energy method. As mentioned previously, the energy method is well explored and offers a convenient way of blade flutter analysis that is computationally inexpensive and can be conducted without advanced high-performance computing (HPC) systems. For careful analysis, each step of this study was either verified or compared with the known data. For example, the modal analysis, the compressor performance, and the flutter analysis (near-peak efficiency region) were thoroughly conducted and verified. Furthermore, in this study, the ability of the energy method to predict the stall flutter onset was also successfully explored. The energy method used in this study predicted the stall flutter onset at -1 nodal diameter. The authors strongly believe that the energy method is sufficient to predict the stall flutter onset with the least computational cost; however, further investigations at this nodal diameter (-1) are inevitable, and a thorough fluid flow phenomenon related to this should be explored further. While the energy method successfully predicted the stall flutter onset, further investigations for the expanded validity of the energy method are mandatory. In addition, the causes of the stall flutter onset and its related flow mechanism should also be investigated in the future. Such aeroelastic (aerodynamic and structural) analyses will also be helpful in understanding the classical question of the relationship between stall inception and flutter, which may include the computationally expensive coupled analysis.

The following conclusions can be drawn from the study:

1. The energy method successfully predicted the stall flutter onset in the transonic compressor.
2. At compressor near-peak efficiency, the energy method predicted the system stability; however, in stall condition, the energy method detected system instability at least for one nodal diameter.
3. Significantly, the prediction of stall flutter onset by the energy method was carried out using the FEM and transient CFD analyses without including any additional or uncommon methods. This computationally inexpensive and time-efficient method provides a wide range of applications for the compressor flutter prediction for future studies.

In the future, further investigations into the expanded validity of the energy method are planned. The relationship between the cause of the stall flutter inception and the related stall flow phenomenon will also be investigated in future studies. The knowledge attained from this study for aerodynamic simulations will be used for designing and simulating enhanced aerodynamic surfaces of sports equipment as a part of the VPP Sports Project.

Author Contributions: Conceptualization, A.A. and A.M.; methodology, A.A. and A.M.; software validation, A.M.; formal analysis, A.A. and A.M.; investigation, A.A. and A.M.; data curation, A.M.;

writing—original draft preparation, A.A.; writing—review and editing, A.A.; visualization, A.M.; supervision, A.A.; and project administration, A.A. All authors have read and agreed to the published version of the manuscript.

Funding: This study is supported by the VPP Sports Project (National Research Program: Sports), and funded by the Ministry of Education and Science and the Latvian Council of Science. Project Nr. VPP-IZM-Sports-2023/1-0001.

Data Availability Statement: The data presented in this study are available on request from the corresponding authors with restrictions as per the discretion of the funding body "Ministry of Education and Science and the Latvian Council of Science".

Acknowledgments: This work is supported by the VPP Sports Project (National Research Program: Sports), and funded by the Ministry of Education and Science and the Latvian Council of Science. Project Nr. VPP-IZM-Sports-2023/1-0001.

Conflicts of Interest: The authors declare no conflicts of interest.

References

1. Casoni, M.; Benini, E. A Review of Computational Methods and Reduced Order Models for Flutter Prediction in Turbomachinery. *Aerospace* **2021**, *8*, 242. [CrossRef]
2. Zheng, Y.; Yang, H. Coupled Fluid-Structure Flutter Analysis of a Transonic Fan. *Chin. J. Aeronaut.* **2011**, *24*, 258–264. [CrossRef]
3. Chen, X.; Zha, G.-C.; Hu, Z. Numerical Simulation of Flow Induced Vibration Based on Fully Coupled Fluid-Structural Interactions. In Proceedings of the 34th AIAA Fluid Dynamics Conference and Exhibit, Portland, OR, USA, 28 June–1 July 2004.
4. Carta, F.O. Coupled Blade-Disk-Shroud Flutter Instabilities in Turbojet Engine Rotors. *J. Eng. Power* **1967**, *89*, 419–426. [CrossRef]
5. Chahine, C.; Verstraete, T.; He, L. A Comparative Study of Coupled and Decoupled Fan Flutter Prediction Methods under Variation of Mass Ratio and Blade Stiffness. *J. Fluids Struct.* **2019**, *85*, 110–125. [CrossRef]
6. Elder, R.; Woods, I.; Patil, S.; Holmes, W.; Steed, R.; Hutchinson, B. Investigation of Efficient CFD Methods for the Prediction of Blade Damping. In Proceedings of the ASME Turbo Expo 2013: Turbine Technical Conference and Exposition, San Antonio, TX, USA, 3–7 June 2013. [CrossRef]
7. Li, H.; Sheng, Z. A Check on the Energy Method of Predicting Blade Transonic Stall Flutter. *Acta Mech. Sin.* **1986**, *2*, 121–128. [CrossRef]
8. Clark, W.S.; Hall, K.C. A Time-Linearized Navier–Stokes Analysis of Stall Flutter. *J. Turbomach.* **1999**, *122*, 467–476. [CrossRef]
9. Ren, J.; Huang, H.; Wang, D.; Dong, X.; Cao, B. An Efficient Coupled-Mode Flutter Analysis Method for Turbomachinery. *Aerosp. Sci. Technol.* **2020**, *106*, 106215. [CrossRef]
10. Šidlof, P.; Šimurda, D.; Lepicovsky, J.; Štěpán, M.; Vomáčko, V. Flutter in a Simplified Blade Cascade: Limits of the Quasi-Steady Approximation. *J. Fluids Struct.* **2023**, *120*, 103913. [CrossRef]
11. Nowinski, M.; Panovsky, J. Flutter Mechanisms in Low Pressure Turbine Blades. *J. Eng. Gas Turbines Power* **1999**, *122*, 82–88. [CrossRef]
12. Srivastava, R.; Bakhle, M.A.; Hoyniak, D. Aeroelastic Analysis of Turbomachinery. *Int. J. Numer. Methods Heat Fluid Flow* **2004**, *14*, 382–402. [CrossRef]
13. Gnesin, V.; Kolodyazhnaya, L.; Rzadkowski, R. Coupled Aeroelastic Oscillations of a Turbine Blade Row in 3D Transonic Flow. *J. Therm. Sci.* **2001**, *10*, 318–324. [CrossRef]
14. Strazisar, A.J.; Powell, J.A. Laser Anemometer Measurements in a Transonic Axial Flow Compressor Rotor. *J. Eng. Power* **1981**, *103*, 430–437. [CrossRef]
15. Roberts, W.B.; Prahst, P.S.; Thorp, S.; Strazisar, A.J. The Effect of Ultrapolish on a Transonic Axial Rotor. In Proceedings of the ASME Turbo Expo 2005: Power for Land Sea, and Air, Reno, NV, USA, 6–9 June 2005; Volume 6. [CrossRef]
16. Arshad, A.; Kovaļčuks, V. Computational investigations for the application of Micro Vortex Generators (MVGs) for 4R-UAV Wing. In Proceedings of the 2023 IEEE Aerospace Conference, Big Sky, MT, USA, 4–9 March 2023; 1095-323X; pp. 1–9. [CrossRef]
17. Arshad, A.; Nawanjana, C.; Kovalcuks, V. Design optimization of low Reynolds number airfoil for enhanced aerodynamics of 4R-UAV. In Proceedings of the 2022 13th International Conference on Mechanical and Aerospace Engineering (ICMAE), Bratislava, Slovakia, 20–22 July 2022; pp. 325–329. [CrossRef]
18. Arshad, A.; Wijesinghe, D.N.; Appuhamila, W.; Kovaļčuks, V. Computational investigations for the application of winglets on small-scale UAVs. In Proceedings of the 2023 International Conference on Military Technologies (ICMT), Brno, Czech Republic, 23–26 May 2023; pp. 1–6. [CrossRef]
19. Arshad, A.; Kovaļčuks, V. Numerical investigations for the influence of shape of trapezoidal Micro Vortex Generators (MVGs) on the aerodynamic performance of the 4R-UAV wing. In Proceedings of the 2023 14th International Conference on Mechanical and Aerospace Engineering (ICMAE), Porto, Portugal, 18–21 July 2023.
20. Arshad, A.; Kovaļčuks, V.; López, I.M. Application of SG6043mod Airfoil for the Enhanced Aerodynamic Characteristics of UAV Wing. In Proceedings of the 2023 10th International Conference on Recent Advances in Air and Space Technologies (RAST), Istanbul, Türkiye, 7–9 June 2023; pp. 1–6. [CrossRef]

21. Erdos, J.I.; Alzner, E.; McNally, W. Numerical Solution of Periodic Transonic Flow through a Fan Stage. *AIAA J.* **1977**, *15*, 1559–1568. [CrossRef]
22. He, L. An Euler Solution for Unsteady Flows around Oscillating Blades. *J. Turbomach.* **1990**, *112*, 714–722. [CrossRef]
23. ANSYS, Inc. *Ansys® CFX, 2022 R2, Help System, CFX User Manual*; ANSYS, Inc.: Canonsburg, PA, USA, 2022.
24. Menter, F.R. Two-Equation Eddy-Viscosity Turbulence Models for Engineering Applications. *AIAA J.* **1994**, *32*, 1598–1605. [CrossRef] [PubMed]